

## SUPPLEMENTARY INFORMATION

### Wavelength-tunable light shaping with cholesteric liquid crystal microlenses

By Chloé Bayon, Gonzague Agez and Michel Mitov\*

Centre d'Elaboration de Matériaux et d'Etudes Structurales (CEMES), CNRS, University Paul-Sabatier,  
29 rue J. Marvig, 31055 Toulouse cedex 4, France.

\*E-mail : mitov@cemes.fr

**This section contains : *Details on numerical simulations and Supplementary figures S1–S3.***

#### Details on numerical simulations

In order to numerically calculate the propagation of light across the material, numerical replica were generated. Meaning that the pitch value, the distribution of the orientation of the helical axis, the spatial resolution and the dielectric birefringence match the experimental features. Simulations were performed by using the finite-difference time-domain (FDTD) method of the Meep<sup>S1</sup> software package. This electromagnetic simulation software uses Maxwell equations and we let them run over time within some finite computational region. The computational grid resolution is 60 pixels per  $\mu\text{m}$ . The 2D box size is 800 pixels along the direction of light propagation and 360 pixels along the transverse direction. We imposed absorbing boundary conditions (the present approach utilizes a setup where the computational cell is surrounded with a medium that absorbs light without any reflection). We set the average refractive index  $n$  at 1.57 and the birefringence  $\Delta n$  at 0.3. The incoming light is a continuous plane wave source proportional to  $\exp(-i\omega t)$  with  $\omega = 2\pi c/\lambda$ , where

$\lambda$  is the wavelength and  $c$  is the speed of light in a vacuum. The polarization is linear and orthogonal to the XZ plane. After a transient regime, 300 images of the electric-field energy density  $\mathbf{E}^* \cdot \mathbf{D}/2$  are recorded during 100 periods. The energy density from both the forward and the backward (due to Bragg reflection) fields are recorded. This quantity oscillates with a pulsation equal to  $2\omega$ . The envelopes are then extracted with a pass band filter centred at  $2\omega$  in the Fourier space. The pictures in Fig. 10 c and d are time averaged over the 100 periods (300 images). The colour scale is proportional to the intensity.

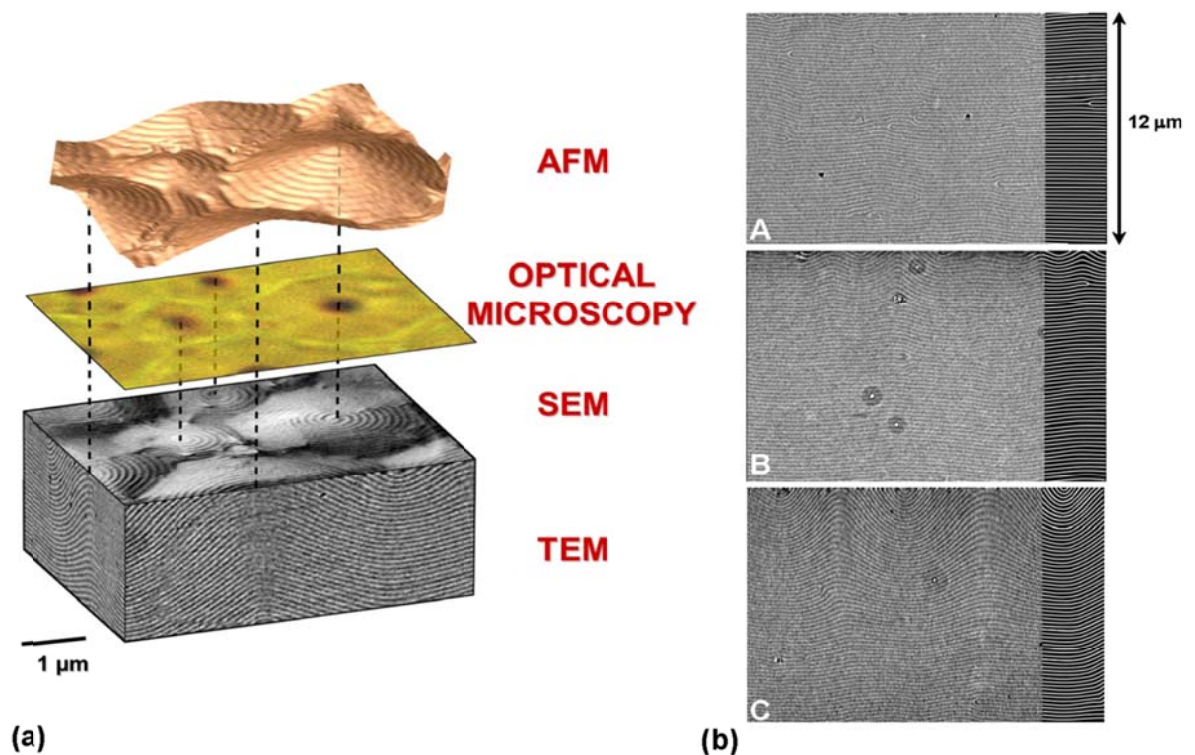


**Fig. S1** Structure of the optical layer. The open cholesteric-liquid-crystalline film was annealed at 140°C for 13 hours, and then quenched at room temperature. It exhibited hybrid anchoring after annealing; meaning the preferential molecular orientation is planar on the glass substrate and it is homeotropic (*i.e.* perpendicular) at the air interface. This hybrid anchoring leads to a specific cellular texture which is called the polygonal texture<sup>24,35</sup>. (a) 3D structure of the polygonal texture according to a combination of the following microscopy methods: atomic force microscopy (AFM), optical

microscopy (OM), scanning electron microscopy (SEM) and transmission electron microscopy (TEM). The micrograph recorded with an optical microscope in transmission mode reveals a mosaic of polygons with various sizes. AFM imaging reveals the cone shape of polygons, which are the locus of double-spiral patterned lines. The connection between oblique lines in the TEM cross-sectional views and spiral patterns as seen in planar views by SEM is visible. Vertical dotted lines help visualize the coincidence between the central spots of cones from one image to the next. The relief of polygons results from the competition between the surface energy and the bulk free energy. The energy is lowered by transforming the free surface into a cone, thus reducing the bulk distortion energy at the cost of surface energy. The double-spiral structures correspond to the adaptation of the cholesteric structure to the relief and the conditions at the limits. A blue shift of the reflection band is caused by the interface-induced variation of the helical axis orientation, which progressively propagates further into the volume as the annealing time increases. (b) TEM images of cross sections of optical layers quenched at 140°C after various annealing times. The right part of each image was redrawn to facilitate the observation of texture changes. (A) No annealing; the fingerprint texture made of an array of periodic bright and dark lines is regularly parallel to both interfaces. The helix axis is perpendicular to the lines everywhere; the distance between two dark (or bright) lines represents the half pitch. (B) Annealing time = 1 min; close to the air interface, the lines undulate, which already shows a change in the orientation of the helix axis. Further down, the lines remain parallel to the surfaces. (C) Annealing time = 13 hours; the distortions invaded the bulk. Only a very thin material thickness close to the substrate exhibits quasi parallel lines.

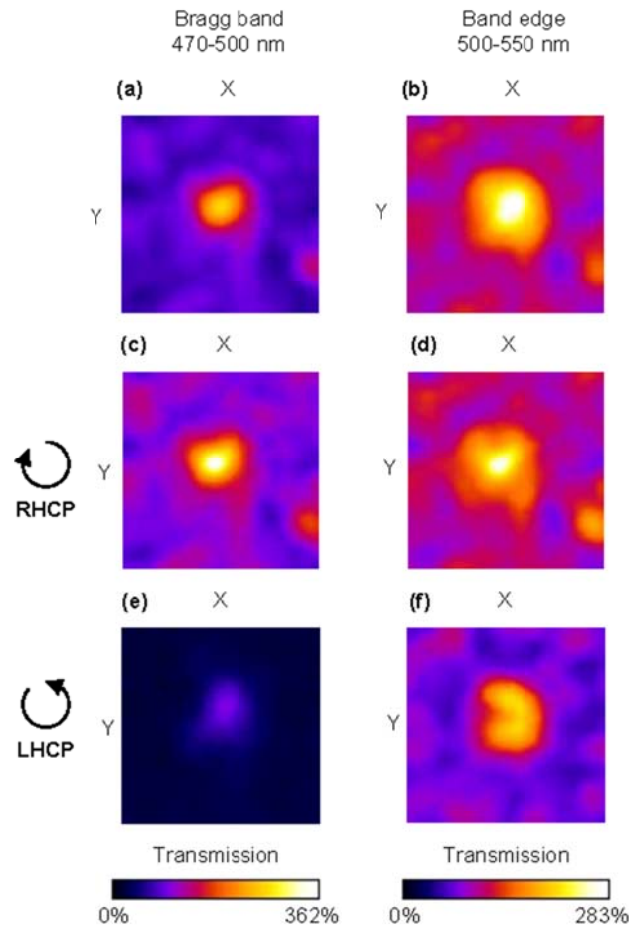


**Fig. S2** Polarization dependent efficiency. Intensity profiles of the transmitted light when the incoming light is: (a-b) unpolarised; (c-d) right-handed circularly polarized (CP); (e-f) left-handed CP. CP light is obtained by combining a linear polarizer with a quarter-wave plate. The transmission rate inside the Bragg band is very weak (e) when the light has the same handedness (*i.e.* left) compared to the helical structure due to the light reflection and the polarization-selectivity rule in CLCs. When the light has the opposite handedness, the spot size is smaller than inside the band edge. When the incoming light is unpolarised, the maximum of efficiency is obtained in the band edge (b).

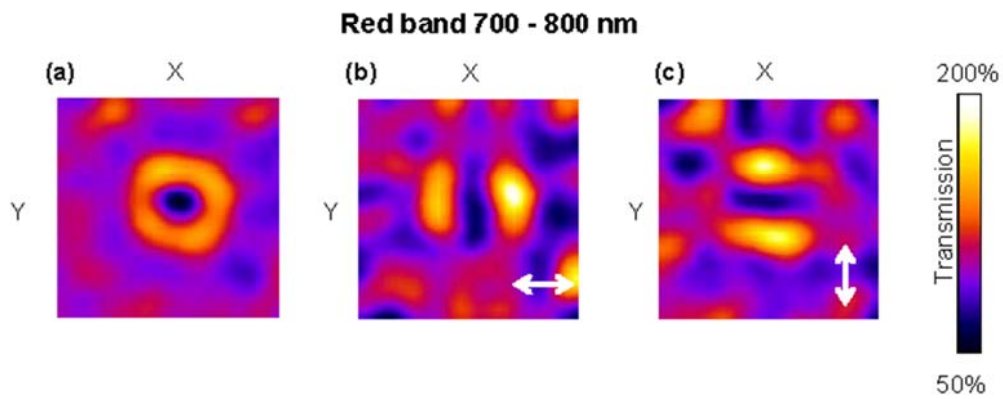


**Fig. S3** Evidence of the radial polarization state of the donut. Intensity profiles at the focal plane in the red band: (a) without analyser; (b) with an x-linear analyser; (c) with a y-linear analyser. The incoming light is unpolarised. The layer was annealed at 140°C for 5 hours. Along the donut ring the polarization is collinear to  $k_{\perp}$ , where  $k_{\perp}$  is the orthogonal component of the Bragg grating wave vector.

S1. F. Ardavan *et al.*, *Comp. Phys. Comm.*, 2010, **181**, 687–702.